

# 1 Measurement report: Oxidation potential of water-soluble 2 aerosol components in the southern and northern of Beijing

3  
4 Wei Yuan<sup>1</sup>, Ru-Jin Huang<sup>1</sup>, Chao Luo<sup>2</sup>, Lu Yang<sup>1</sup>, Wenjuan Cao<sup>1</sup>, Jie Guo<sup>1</sup>, Huinan  
5 Yang<sup>2</sup>

6  
7 <sup>1</sup>State Key Laboratory of Loess and Quaternary Geology, Center for Excellence in  
8 Quaternary Science and Global Change, Institute of Earth Environment, Chinese  
9 Academy of Sciences, Xi'an 710061, China.

10 <sup>2</sup>School of Energy and Power Engineering, University of Shanghai for Science and  
11 Technology, Shanghai 200093, China

12 Correspondence: Ru-Jin Huang (rujin.huang@ieecas.cn) and Huinan Yang  
13 (yanghuinan@usst.edu.cn)

## 14 15 Abstract

16 Water-soluble components have significant contribution to the oxidative  
17 potential (OP) of atmospheric fine particles (PM<sub>2.5</sub>), while our understanding of  
18 water-soluble PM<sub>2.5</sub> OP and its sources, as well as its relationship with water-soluble  
19 components, is still limited. In this study, the water-soluble OP levels in wintertime  
20 PM<sub>2.5</sub> in the south and north of Beijing, representing the difference in sources, were  
21 measured with dithiothreitol (DTT) assay. The volume normalized DTT (DTT<sub>v</sub>) in the  
22 north ( $3.5 \pm 1.2 \text{ nmol min}^{-1} \text{ m}^{-3}$ ) was comparable to that in the south ( $3.9 \pm 0.9 \text{ nmol}$   
23  $\text{min}^{-1} \text{ m}^{-3}$ ), while the mass normalized DTT (DTT<sub>m</sub>) in the north ( $65.3 \pm 27.6 \text{ pmol}$   
24  $\text{min}^{-1} \mu\text{g}^{-3}$ ) was almost twice that in the south ( $36.1 \pm 14.5 \text{ pmol min}^{-1} \mu\text{g}^{-3}$ ). In both  
25 the south and north of Beijing, DTT<sub>v</sub> was better correlated with soluble elements  
26 instead of total elements. In the north, soluble elements (mainly Mn, Co, Ni, Zn, As,  
27 Cd and Pb) and water-soluble organic compounds, especially light-absorbing  
28 compounds (also known as brown carbon), had positive correlations with DTT<sub>v</sub>.

29 However, in the south, the  $DTT_v$  was mainly related to soluble As, Fe and Pb. The  
30 sources of  $DTT_v$  were further resolved using the positive matrix factorization (PMF)  
31 model. Traffic-related emissions (39.1%) and biomass burning (25.2%) were the main  
32 sources of  $DTT_v$  in the south, and traffic-related emissions (> 50%) contributed the  
33 most of  $DTT_v$  in the north. Our results indicate that vehicle emission was the  
34 important contributor to OP in Beijing ambient  $PM_{2.5}$  and suggest that more study is  
35 needed to understand the intrinsic relationship between OP and light absorbing  
36 organic compounds.

37

## 38 **1 Introduction**

39 Atmospheric fine particulate matter ( $PM_{2.5}$ ) pollution is one of the major global  
40 environmental issues, affecting air quality, climate and human health (Huang et al.,  
41 2014; Burnett et al., 2018; An et al., 2019; Zheng et al., 2020). The exposure to  $PM_{2.5}$   
42 was estimated to be responsible for 8.9 million deaths worldwide in 2015, of which  
43 28% occurred in China (Burnett et al., 2018). Numerous studies have shown that  
44 oxidative stress is one of the main mechanisms underlying the adverse effects of  
45  $PM_{2.5}$  on human health (Chowdhury et al., 2019; Lelieveld et al., 2021; Yu et al.,  
46 2022b). When entering the human body,  $PM_{2.5}$  can induce the production of excessive  
47 reactive oxygen species (ROS) (e.g.,  $H_2O_2$ ,  $\cdot OH$  and  $\cdot O_2^-$ ), leading to cellular redox  
48 imbalance and generating oxidative stress effects. The ability of  $PM_{2.5}$  to cause  
49 oxidative stress is defined as oxidative potential (OP).

50 The methods to determine the OP of  $PM_{2.5}$  include cellular and acellular assays,  
51 and acellular methods are more widely used than cellular methods (Charrier and  
52 Anastasio, 2012; Xiong et al., 2017; Calas et al., 2018; Bates et al., 2019; Wang et al.,  
53 2020b; Campbell et al., 2021; Oh et al., 2023). Among acellular methods, the  
54 dithiothreitol (DTT) assay is extensively applied to determine the OP of ambient  
55 particles (Charrier and Anastasio, 2012; Xiong et al., 2017; Liu et al., 2018; Wang et  
56 al., 2020b; Puthussery et al., 2022; Wu et al., 2022a). DTT is a surrogate of cellular  
57 reductants, and the consumption rate of DTT was used to assess the OP of  $PM_{2.5}$ .

58 Previous studies have shown that organic matters (e.g., water-soluble organic species  
59 and PAHs) and some transition metals (e.g., Mn and Cu) are the important  
60 contributors to DTT consumption of PM<sub>2.5</sub> (Charrier and Anastasio, 2012; Verma et al.,  
61 2015; Bates et al., 2019; Wu et al., 2022a; Wu et al., 2022b). For example, Charrier  
62 and Anastasio (2012) measured the OP of PM<sub>2.5</sub> in San Joaquin Valley, California and  
63 reported that about 80% of DTT consumption was contributed by transition metals.  
64 Verma et al. (2015) measured the OP of water-soluble PM<sub>2.5</sub> in the southeastern  
65 United States and reported that about 60% of DTT activity was contributed by water-  
66 soluble organics. The mixtures of metals and organics may produce synergistic or  
67 antagonistic effects, such as  $\cdot\text{O}_2^-$  produced from oxidation of DTT by quinones is  
68 more efficiently transformed to  $\cdot\text{OH}$  in the presence of Fe, while the DTT  
69 consumption and  $\cdot\text{OH}$  generation of quinones are reduced in the presence of Cu  
70 (Xiong et al., 2017; Yu et al., 2018; Bates et al., 2019).

71 A number of studies have investigated the OP of water-soluble components in  
72 PM<sub>2.5</sub>, which show that the average water-soluble OP values in urban areas ranged  
73 from 0.1 to 10 nmol min<sup>-1</sup> m<sup>-3</sup> (Fang et al., 2016; Liu et al., 2018; Chen et al., 2019;  
74 Wu et al., 2022a; Yu et al., 2022a; Xing et al., 2023). Due to the complexity in  
75 chemical composition and sources of PM<sub>2.5</sub> that determine the OP levels, the sources  
76 of OP are also diverse (Verma et al., 2015; Bates et al., 2019; Tuet et al., 2019; Yu et  
77 al., 2019; Cao et al., 2021). Several studies have investigated the emission sources and  
78 ambient samples to identify the sources of OP (Tuet et al., 2019; Yu et al., 2019; Wang  
79 et al., 2020b; Cao et al., 2021), which include both primary and secondary sources.  
80 For example, Cao et al. (2021) measured the water-soluble OP of PM<sub>2.5</sub> samples from  
81 six biomass and five coal burning emissions in China, with average values of 4.5-7.4  
82 and 0.5-2.1 pmol min<sup>-1</sup>  $\mu\text{g}^{-1}$ , respectively. Tong et al. (2018) investigated the OP of  
83 secondary organic aerosols (SOA) from oxidation of naphthalene, isoprene and  $\beta$ -  
84 pinene with  $\cdot\text{OH}$  or O<sub>3</sub>, which were  $104.4 \pm 7.6$ ,  $48.3 \pm 7.9$  and  $36.4 \pm 3.1$  pmol min<sup>-1</sup>  
85  $\mu\text{g}^{-1}$ , respectively. Verma et al. (2014) identified the source of water-soluble OP of  
86 PM<sub>2.5</sub> in Atlanta, United States from June 2012 to September 2013 with positive

87 matrix factorization (PMF) and chemical mass balance (CMB) methods, of which  
88 biomass burning was the largest contributor. Wang et al. (2020b) quantified the  
89 sources of water-soluble OP of PM<sub>2.5</sub> in Xi'an, China in 2017 using PMF and multiple  
90 linear regression (MLR) methods, with significant contributions from secondary  
91 sulfates, vehicle emissions and coal combustion. Despite these efforts, comparative  
92 studies on the differences in pollution levels and sources of PM<sub>2.5</sub> OP in different  
93 districts are still limited.

94 In this study, the DTT activity of water-soluble matter in PM<sub>2.5</sub> samples collected  
95 simultaneously in the southern and northern of Beijing in January 2018 were  
96 measured. The concentration and light absorption of water-soluble organic carbon  
97 (WSOC), as well as the concentrations of 14 trace elements and 7 light-absorbing  
98 nitroaromatic compounds (NACs) were quantified. The sources of DTT activity were  
99 then identified with PMF model. The results acquired in this study provide a  
100 comparison of PM<sub>2.5</sub> OP in different districts of Beijing and its connection with  
101 organic compounds, trace elements and sources, which could be helpful for further  
102 study of the regional differences in the effects of PM<sub>2.5</sub> on human health.

103

## 104 **2 Materials and methods**

### 105 **2.1 Sampling**

106 Ambient 24 h integrated PM<sub>2.5</sub> filter samples were collected from January 1 to 31,  
107 2018 simultaneously in the south (the Dingfuzhuang village (DFZ), Daxing district;  
108 39.61°N, 116.28°E) and north (the National Center for Nanoscience and Technology  
109 (NCNT), Haidian district; 39.99°N, 116.32°E) of Beijing (Figure S1). The distance  
110 between the two sampling sites is about 42 km. The south site is surrounded by  
111 agricultural, industrial, and transportation areas, and the north site is surrounded by  
112 residential, transportation and commercial areas. PM<sub>2.5</sub> samples were collected on pre-  
113 baked (780 °C, 3 h) quartz-fiber filters (20.3 × 25.4 cm; Whatman, QM-A, Clifton, NJ,  
114 USA) using high-volume PM<sub>2.5</sub> samplers (1.13 m<sup>3</sup> min<sup>-1</sup>; Tisch, Cleveland, OH, USA)  
115 which were placed on the roof of buildings at heights of about 5 m (south) and 20 m

116 (north) above the ground. 31 samples were collected at each site. After collection, the  
117 samples were wrapped in baked aluminum foils and stored in a freezer ( $-20\text{ }^{\circ}\text{C}$ ) until  
118 further analysis.

## 119 **2.2 Chemical analysis**

120 The mass of  $\text{PM}_{2.5}$  on the filter was measured by a digital microbalance with a  
121 precision of 0.1 mg (LA130S-F, Sartorius, Germany) after 24-h equilibration at a  
122 constant temperature ( $20\text{-}23\text{ }^{\circ}\text{C}$ ) and humidity (35-45%) chamber. Each filter was  
123 weighted at least two times, and the deviations for blank and sampled filters among  
124 the repetitions were less than 5 and 10  $\mu\text{g}$ , respectively. The  $\text{PM}_{2.5}$  mass concentration  
125 was calculated by dividing the weight difference before and after sampling by the  
126 volume of sampled air.

127 For WSOC analysis, one punch ( $1.5\text{ cm}^2$  for concentration analysis and  $0.526$   
128  $\text{cm}^2$  for light absorption measurement) of filter was taken from each sample and  
129 extracted ultrasonically with ultrapure water ( $> 18.2\text{ M}\Omega\text{ cm}$ ) for 30 min. After, the  
130 extracts were filtered with a  $0.45\text{ }\mu\text{m}$  PVDF pore syringe filter to remove insoluble  
131 substances. Finally, the concentration of WSOC was measured with a total organic  
132 carbon-total nitrogen analyzer (TOC-L, Shimadzu, Japan; (Ho et al., 2015)) and the  
133 light absorption of WSOC was measured by an UV-Vis spectrophotometer (300-700  
134 nm; Ocean Optics, USA) equipped with a liquid waveguide capillary cell (LWCC-  
135 3100, World Precision Instruments, Sarasota, FL, USA; (Yuan et al., 2020)). The  
136 absorption coefficient (Abs) of WSOC was calculated according to formula S1 in the  
137 Supporting Information (SI).

138 The total concentration and soluble fraction concentration of 14 trace elements  
139 (i.e., Ti, V, Cr, Mn, Fe, Co, Ni, Cu, Zn, As, Sr, Cd, Ba, and Pb) were quantified by an  
140 inductively coupled plasma mass spectrometer (ICP-MS, 7700x, Agilent Technologies,  
141 USA), and the details are shown in the SI. For soluble fraction concentration analysis,  
142 a punch of filter (47 mm diameter) was extracted with ultrapure water and then  
143 centrifuged from residues. For total concentration analysis, another 47 mm diameter  
144 filter of the same sample was used and digested with 10 mL  $\text{HNO}_3$  and 1 mL HF at

145 180 °C for 12 h. The extracts were then heated and concentrated to ~ 0.1 mL, and  
146 diluted to 5 mL with 2% HNO<sub>3</sub>. Afterwards, the diluents were filtered with a 0.22 µm  
147 PTFE pore syring filter and stored in a freezer (-4 °C) until further ICP-MS analysis.

148 The concentrations of organic markers (including levoglucosan, mannosan,  
149 galactosan, hopanes (including 17α(H)-22,29,30-trisnorhopane, 17α(H),21β(H)-30-  
150 norhopane, 17β(H),21α(H)-30-norhopane, 17β(H),21α(H)-hopane, 17β(H),21α(H)-  
151 hopane and 17β(H),21α(H)-hopane), picene, phthalic acid, isophthalic acid and  
152 terephthalic acid) and light-absorbing NACs (including 4-nitrophenol (4NP), 2-  
153 methyl-4-nitrophenol (2M4NP), 3-methyl-4-nitrophenol (3M4NP), 4-nitrocatechol  
154 (4NC), 3-methyl-5-nitrocatechol (3M5NC), 4-methyl-5-nitrocatechol (4M5NC) and  
155 4-nitro-1-naphthol (4N1N)) were determined by a gas chromatograph–mass  
156 spectrometer (GC-MS; Agilent Technologies, Santa Clara, CA, USA) following the  
157 method described elsewhere (Wang et al., 2020a), and more details about the analysis  
158 can be found in SI. All of the results reported in this study were corrected for blanks.

### 159 **2.3 Oxidative potential**

160 The DTT assay was applied to determine the oxidative potential of water-soluble  
161 components in PM<sub>2.5</sub> according to the method by Gao et al. (2017). In brief, a quarter  
162 of a 47 mm filter was ultrasonically extracted with 5 mL ultrapure water for 30 min  
163 and then filtered with a 0.45 µm PVDF pore syring filter to remove insoluble  
164 substances. Several studies have shown that ultrasonic treatment of samples can lead  
165 to an increase in its OP values (Miljevic et al., 2014; Jiang et al., 2019), however,  
166 there was also a study showed that the difference in OP values of water-soluble PM<sub>2.5</sub>  
167 measured by DTT assay was little for samples extracted by ultrasonic and shaking  
168 (Gao et al., 2017). Consistent with the extraction methods of organic markers and  
169 trace elements analysis, ultrasonic method was used to extract samples for DTT  
170 analysis. Afterwards, 0.5 mL of the extract was mixed with 1 mL of potassium  
171 phosphate buffer (pH = 7.4) and 0.5 mL of 2 mM DTT in a brown vial, and then  
172 placed in a water bath at 37 °C. Then, 20 µL of this mixture was taken at designated  
173 time intervals (2, 7, 13, 20, and 28 min) and mixed with 1 mL trichloroacetic acid

174 (TCA; 1% w/v) in another brown vial to terminate the reaction. Then, 0.5 mL of 5,5'-  
175 dithiobis-(2-nitrobenzoic acid) (DTNB; 2.5  $\mu\text{M}$ ) and 2 mL of tris buffer (pH = 8.9)  
176 were added to form 2-nitro-5-thiobenzonic acid (TNB) which has light absorption at  
177 412 nm. Finally, the absorption of TNB was measured by a LWCC-UV-Vis. The DTT  
178 consumption rate was quantified by the remaining DTT concentration at different  
179 reaction times. Daily solution blanks and filter blanks were analyzed in parallel with  
180 samples to evaluate the consistency of the system performance. Ambient samples  
181 were corrected for filter blank. The DTT activities were normalized by the volume of  
182 sampled air ( $\text{DTT}_v$ ,  $\text{nmol min}^{-1} \text{m}^{-3}$ ) and the mass concentration of  $\text{PM}_{2.5}$  ( $\text{DTT}_m$ ,  $\text{pmol}$   
183  $\text{min}^{-1} \mu\text{g}^{-1}$ ).

184 Considering that for samples with significant contributions from species whose  
185 DTT response is non-linear related to  $\text{PM}_{2.5}$  mass (e.g., Cu, Mn), the  $\text{DTT}_m$  value  
186 depends on the concentration of  $\text{PM}_{2.5}$  in the extraction solution (Charrier et al., 2016).  
187 The response of  $\text{DTT}_m$  to  $\text{PM}_{2.5}$  concentration in the extraction solution was analyzed  
188 using sample with high concentrations of soluble Cu and Mn (Figure S2). In the range  
189 of  $\text{PM}_{2.5}$  concentrations less than 150  $\mu\text{g mL}^{-1}$ , the  $\text{DTT}_m$  response was greatly  
190 affected by  $\text{PM}_{2.5}$  concentrations, however, when the concentrations of  $\text{PM}_{2.5}$  in the  
191 extract were greater than 150  $\mu\text{g mL}^{-1}$ , the  $\text{DTT}_m$  response changed little (< 12%) with  
192 the increase of  $\text{PM}_{2.5}$  concentrations. In this study, the concentrations of  $\text{PM}_{2.5}$  in the  
193 extraction solution of most samples from the two sites were greater than 150  $\mu\text{g mL}^{-1}$   
194 (ranged from 78.7 to 748.7  $\mu\text{g mL}^{-1}$ , with average values of  $408.9 \pm 164.1$  and  $206.6 \pm$   
195  $95.0 \mu\text{g mL}^{-1}$  in the south and north, respectively), therefore, the difference in  $\text{PM}_{2.5}$   
196 concentrations in different sample extracts should had a relatively small impact on the  
197 difference in  $\text{DTT}_m$  values of the samples. This study did not consider the impact of  
198 metal precipitation in phosphate matrix on the measured DTT values, as there is no a  
199 straightforward method to correct the artifacts caused by this phenomenon  
200 (Yalamanchili et al., 2023).

## 201 **2.4 Source apportionment**

202 The sources of DTT activities were identified and quantified using PMF model

203 implemented by the multilinear engine (ME-2; (Paatero, 1997)) following the method  
204 described in our previous studies (Huang et al., 2014; Yuan et al., 2020). A total of 62  
205 samples and 23 species were input into PMF model. The number of samples is higher  
206 than the number of species, and approaching the ratio of at least 3:1 proposed by Belis  
207 et al. (2019). The input data include species concentration (including DTT<sub>v</sub>, 14 trace  
208 elements and 8 organic markers) and uncertainties. The species-specific uncertainties  
209 were calculated following Liu et al. (2017). More details are described in SI (PMF  
210 analysis).

211

## 212 **3 Results and discussion**

### 213 **3.1 DTT activity and concentrations of water-soluble PM<sub>2.5</sub> components**

214 Figure 1 shows the daily variation of DTT activity, light absorption of WSOC at  
215 wavelength 365 nm (Abs<sub>365</sub>), together with the concentrations of PM<sub>2.5</sub>, WSOC,  
216 NACs and total elements in the south and north of Beijing. Their average values are  
217 shown in Table S1. Generally, the average values of PM<sub>2.5</sub>, WSOC, Abs<sub>365</sub>, NACs and  
218 total elements were higher in the south than in the north. Specifically, the  
219 concentrations of PM<sub>2.5</sub> and WSOC in the south ( $122.3 \pm 48.9 \mu\text{g m}^{-3}$  and  $8.1 \pm 5.0$   
220  $\mu\text{gC m}^{-3}$ , respectively) were both about two times higher than that in the north ( $62.3 \pm$   
221  $27.9 \mu\text{g m}^{-3}$  and  $4.0 \pm 2.0 \mu\text{gC m}^{-3}$ , respectively), indicating that the proportion of  
222 WSOC in PM<sub>2.5</sub> was similar in the south and north. However, the Abs<sub>365</sub> in the south  
223 was about three times that in the north, indicating that the chemical composition of  
224 WSOC was different between the south and north. Previous studies have reported that  
225 NACs are the main water-soluble light-absorbing organic compounds (also known as  
226 brown carbon, BrC) of PM<sub>2.5</sub> (Lin et al., 2017; Huang et al., 2020; Li et al., 2020). For  
227 the 7 NACs quantified in this study, the total concentration of nitrophenols (4NP,  
228 2M4NP and 3M4NP), nitrocatechols (4NC, 3M5NC and 4M5NC), and 4N1N in the  
229 south ( $108.5 \pm 72.9 \text{ ng m}^{-3}$ ,  $118.5 \pm 91.5 \text{ ng m}^{-3}$  and  $12.4 \pm 8.2 \text{ ng m}^{-3}$ , respectively)  
230 was about three, five and four times, respectively, those in the north ( $35.5 \pm 21.7 \text{ ng}$   
231  $\text{m}^{-3}$ ,  $24.1 \pm 30.4 \text{ ng m}^{-3}$  and  $3.1 \pm 3.0 \text{ ng m}^{-3}$ , respectively). These results indicate that



232 the sources and emission strength of water-soluble organic compounds were different  
233 in the south and north of Beijing, suggesting the different contribution of water-  
234 soluble organic compounds to DTT activity. The concentration trend of elements was  
235 also different between the south and north of Beijing, with Fe > Zn > Ti > Mn > Cu >  
236 Ba > Pb > Sr > Cr > As > V > Ni > Cd > Co in the south, and Fe > Ti > Zn > Ba >  
237 Mn > Pb > Cu > Cr > Sr > As > Ni > V > Cd > Co in the north. It should be noted that  
238 although the content of PM<sub>2.5</sub>, WSOC and total elements measured in this study were  
239 higher in the south than in the north, the average DTT<sub>v</sub> value in the south ( $3.9 \pm 0.9$   
240  $\text{nmol min}^{-1} \text{m}^{-3}$ ) was comparable to that in the north ( $3.5 \pm 1.2 \text{ nmol min}^{-1} \text{m}^{-3}$ ),  
241 meanwhile, the average DTT<sub>m</sub> value was much higher (1.8 times) in the north ( $65.3 \pm$   
242  $27.6 \text{ pmol min}^{-1} \mu\text{g}^{-1}$ ) than in the south ( $36.1 \pm 14.5 \text{ pmol min}^{-1} \mu\text{g}^{-1}$ ). The lower  
243 DTT<sub>m</sub> in the south than in the north may be due to the increased PM<sub>2.5</sub> in the south  
244 containing more substances with no or little contribution to DTT activity, and  
245 indicates that the intrinsic OP of water-soluble components of PM<sub>2.5</sub> was higher in the  
246 north than in the south. The similar DTT<sub>v</sub> values in the south and north indicate that  
247 the exposure-relevant OP of water-soluble components of PM<sub>2.5</sub> was comparable in  
248 the two sites, and the water-soluble DTT<sub>v</sub> was not consistent with the content of  
249 water-soluble substances.

250 Figure 2 shows the comparison of water-soluble PM<sub>2.5</sub> DTT activity measured in  
251 this study with those measured in other regions of Asia during similar periods. It can  
252 be seen that the DTT<sub>v</sub> values measured in Beijing in this study were lower than that in  
253 Jinzhou, Tianjin, Yantai, and Shanghai in China, Lahore and Peshawar in Pakistan,  
254 and Delhi in India (Liu et al., 2018; Ahmad et al., 2021; Puthussery et al., 2022; Wu et  
255 al., 2022a), higher than that in Xi'an, Nanjing, Hangzhou, Guangzhou, and Shenzhen  
256 in China (Wang et al., 2019; Wang et al., 2020b; Ma et al., 2021; Yu et al., 2022c;  
257 Xing et al., 2023), and comparable with that in Ningbo, China (Chen et al., 2022).  
258 Different from DTT<sub>v</sub>, the DTT<sub>m</sub> value measured in NCNT in Beijing was similar with  
259 that in Jinzhou, Tianjin, Yantai, Shanghai and Ningbo in China (Liu et al., 2018; Chen  
260 et al., 2022; Wu et al., 2022a), and higher than that in other regions. The differences in

261 water-soluble DTT activity of PM<sub>2.5</sub> in different regions can be explained by the  
262 differences in chemical composition, sources and atmospheric formation processes  
263 (Tong et al., 2017; Wong et al., 2019; Daellenbach et al., 2020; Wang et al., 2020b;  
264 Cao et al., 2021). For example, Cao et al. (2021) reported the water-soluble DTT  
265 activity of PM<sub>2.5</sub> from biomass and coal burning emissions in China, and the average  
266 value of biomass burning (4.5-7.4 pmol min<sup>-1</sup> μg<sup>-1</sup>) was much higher than that of coal  
267 burning (0.5-2.1 pmol min<sup>-1</sup> μg<sup>-1</sup>). Tuet et al. (2017) measured the water-soluble DTT  
268 activity of SOA generated under different precursors and reaction conditions, with  
269 SOA from naphthalene photooxidation under RO<sub>2</sub> + NO-dominant dry reaction  
270 conditions had the highest DTT activity.

### 271 **3.2 Correlation between DTT activity and water-soluble PM<sub>2.5</sub> components**

272 Figure 3 shows the correlations of DTT<sub>v</sub> with PM<sub>2.5</sub>, WSOC and Abs<sub>365</sub> in the  
273 south and north of Beijing. It can be seen that the correlation coefficient between  
274 DTT<sub>v</sub> and PM<sub>2.5</sub> was moderate in both the south (r = 0.42) and north (r = 0.45),  
275 indicating that the toxicity of particles can not be evaluated solely by the total PM<sub>2.5</sub>  
276 concentration. The correlations between DTT<sub>v</sub> with WSOC and Abs<sub>365</sub> were strong in  
277 the north (r of 0.69 and 0.70, respectively), while relatively weak in the south (r of  
278 0.41 and 0.40, respectively). The high correlations between DTT<sub>v</sub> with WSOC and  
279 Abs<sub>365</sub> in the north of Beijing qualitatively agree with previous studies in Xi'an, China  
280 and Atlanta, United States (Verma et al., 2012; Chen et al., 2019), and suggest that  
281 water-soluble organic matter, especially BrC, has a significant contribution to DTT  
282 consumption in the north. Light-absorbing BrC typically has conjugated electrons,  
283 making it more likely to transport electrons for catalytic reactions, thereby  
284 contributing to DTT activity (Chen et al., 2019; Wu et al., 2022). Further, in the north,  
285 the DTT<sub>v</sub> was closely related to the concentrations of NACs (r of 0.57 to 0.79) (Figure  
286 S3), suggesting that NACs may be important contributors to DTT consumption. Feng  
287 et al. (2022) reported the positive correlations between NACs and biomarkers in  
288 saliva and urine (interleukin-6 and 8-hydrox-2'-deoxyguanosine). Zhang et al. (2023)  
289 also reported that NACs are major proinflammatory components in organic aerosols,

290 contributing about 24% of the interleukin-8 response of all compounds detected by  
291 Fourier transform ion cyclotron resonance mass spectrometry (FT-ICR-MS) in  
292 electrospray ionization negative mode (ESI-). Certainly, it may also be other  
293 substances related to NACs that contribute to the DTT activity, including those not  
294 detected in this study, driving the good correlation between NACs and DTT<sub>v</sub> in the  
295 north of Beijing, which is worth studying in the future.

296 The correlation coefficients between DTT<sub>v</sub> and 14 trace elements are shown in  
297 Figure 4. Generally, the correlations between DTT<sub>v</sub> and soluble elements were higher  
298 than that between DTT<sub>v</sub> and total elements in both the south and north of Beijing. For  
299 soluble elements, in the south, the DTT<sub>v</sub> showed positive correlations with Mn, Fe, Cr,  
300 Co, As and Pb ( $r > 0.5$ ), while in the north, it exhibited strong positive correlations  
301 with Mn, Co, Ni, Zn, As, Cd and Pb ( $r > 0.7$ ), indicating the different sources of DTT<sub>v</sub>  
302 in the south and north of Beijing. It is worth noting that the concentrations of all  
303 soluble elements were higher in the south than in the north (Figure S4), while the  
304 correlation between DTT<sub>v</sub> and most soluble elements was lower in the south than in  
305 the north (Figure 4). The high correlations between DTT<sub>v</sub> and soluble elements in the  
306 north of Beijing suggests that soluble elements also had significant contribution to  
307 DTT consumption. The low correlations between DTT<sub>v</sub> and soluble elements in the  
308 south of Beijing may be due to the nonlinear relationship between DTT consumption  
309 and elements concentrations (Charrier and Anastasio, 2012; Wu et al., 2022a).

310 In addition to being associated with individual water-soluble species, the  
311 interaction between metal and organic compounds also affects the consumption of  
312 DTT (Xiong et al., 2017; Wu et al., 2022b), with both synergistic and antagonistic  
313 effects. For example, Wu et al. (2022b) measured the DTT consumption of Fe(III) and  
314 Cu(II) interacting with 1,4-naphthoquinone, 9,10-phenanthraquinone, citric acid, and  
315 4-nitrocatechol, respectively. Their results showed that Cu(II) had antagonistic effects  
316 in interacting with most organics except for citric acid, and Fe(III) had an additive  
317 effect on DTT consumption of 1,4-naphthoquinone and citric acid, while it had an  
318 antagonistic effect on 1,4-naphthoquinone and 9,10-phenanthraquinone. Due to the

319 complex composition of water-soluble organic aerosols, the knowledge about the  
320 effects of organics and metal-organic interactions on DTT activity are still limited,  
321 especially the effects of BrC chromophores and their interactions with metals.

### 322 **3.3 Sources of DTT activity**

323 This study analyzed eight organic markers (including levoglucosan, mannosan,  
324 and galactosan for biomass burning, hopanes for vehicle emissions, picene for coal  
325 combustion, and phthalic acid, isophthalic acid and terephthalic acid for secondary  
326 formation) to help identify the sources of DTT activity. The correlation coefficients  
327 between  $DTT_v$  and organic markers are shown in Figure S5. In the south,  
328 levoglucosan, mannosan, galactosan, and hopanes had moderate correlation with  
329  $DTT_v$  (r of 0.41 to 0.48); phthalic acid, isophthalic acid and terephthalic acid had low  
330 to moderate correlation with  $DTT_v$  (r of 0.28 to 0.54); picene had low correlation with  
331  $DTT_v$  (r of 0.21). These results suggest that biomass burning and vehicle emissions  
332 could have significant contribution to water-soluble  $PM_{2.5}$  OP in the south. In the  
333 north, hopanes had the highest correlation with  $DTT_v$  ( $r = 0.70$ ), indicating that  
334 vehicle emissions could have an important contribution. Levoglucosan, mannosan,  
335 galactosan, phthalic acid, isophthalic acid, terephthalic acid, and picene had moderate  
336 to high correlations with  $DTT_v$  in the north, suggesting that biomass and coal burning,  
337 and secondary formation may also have certain contribution to water-soluble  $PM_{2.5}$   
338 OP.

339 To further quantify the sources of DTT activity in the south and the north of  
340 Beijing, the PMF model, which was widely used for the source apportionment of  
341  $PM_{2.5}$  OP (Liu et al., 2018; Shen et al., 2022; Cui et al., 2023), was applied. The input  
342 species include  $DTT_v$ , soluble elements and organic markers, and five to seven factors  
343 were examined. Due to the oil factor mixed with vehicle emissions factor in the five-  
344 factor solution, and there was no new reasonable factor when increasing the factor  
345 number to seven in the PMF analysis (Figure S6). Finally, six factors were resolved  
346 and quantified using PMF model in the south and north of Beijing, including biomass  
347 burning, coal burning, traffic-related, dust, oil combustion, and secondary formation,

348 and the profiles of these sources are shown in Figure S7. Factor 1 is characterized by  
349 high contribution of levoglucosan, mannosan, and galactosan, mainly from biomass  
350 burning (Huang et al., 2014; Chow et al., 2022). The DTT activity of biomass burning  
351 organic aerosol was measured by Wong et al. (2019), which was  $48 \pm 6 \text{ pmol min}^{-1}$   
352  $\mu\text{g}^{-1}$  of WSOC. Liu et al. (2018) quantified the sources of  $\text{DTT}_v$  in coastal cities  
353 (Jinzhou, Tianjin, and Yantai) in China with PMF model and multiple linear  
354 regression method, and the results showed that biomass burning contributed 27.8% on  
355 average in winter. Factor 2 exhibits a large fraction of picene, Zn, Mn, Cd, As, and Pb,  
356 which is considered to be coal burning (Huang et al., 2014; Huang et al., 2018). Joo et  
357 al. (2018) measured the DTT activity of  $\text{PM}_{2.5}$  emitted from coal combustion at  
358 different temperatures, with the highest values of  $26.2 \pm 20.5 \text{ pmol min}^{-1} \mu\text{g}^{-1}$  and  $0.10$   
359  $\pm 0.06 \text{ nmol min}^{-1} \text{ m}^{-3}$  occurring at 550 °C. Factor 3 is identified as traffic-related  
360 emissions, which is characterized by the higher loading of hopanes, Ba, Sr, Cu and Ni  
361 (Huang et al., 2018; Chow et al., 2022). Vreeland et al. (2017) measured the DTT  
362 activity of  $\text{PM}_{2.5}$  emitted by side street and highway vehicles in Atlanta, with values of  
363  $0.78 \pm 0.60 \text{ nmol min}^{-1} \text{ m}^{-3}$  and  $1.08 \pm 0.60 \text{ nmol min}^{-1} \text{ m}^{-3}$ , respectively. Ting et al.  
364 (2023) reported that the DTT activity of  $\text{PM}_{2.5}$  from vehicle emissions in Ziqing  
365 tunnel in Taiwan, China, was 0.15-0.46  $\text{nmol min}^{-1} \text{ m}^{-3}$ . Factor 4, secondary formation,  
366 which is identified by high levels of phthalic acid, isophthalic acid, and terephthalic  
367 acid (Al-Naiema and Stone, 2017; Wang et al., 2020a). Verma et al. (2014) reported  
368 that secondary formation contributed about 30% to the water-soluble DTT activity of  
369  $\text{PM}_{2.5}$  in urban Atlanta. It is worth noting that the DTT activity of SOA generated  
370 from different precursors is different (Tuet et al., 2017; Tong et al., 2018). For  
371 example, the DTT activity of SOA from naphthalene was higher than that from  
372 isoprene (Tuet et al., 2017; Tong et al., 2018). Factor 5 is dominated by crustal  
373 elements Fe and Ti, mainly from dust (Huang et al., 2018). The DTT activity of  
374 atmospheric particulate matter during dust periods were reported in previous studies  
375 (Chirizzi et al., 2017; Khoshnamvand et al., 2023) and it has a low contribution in this  
376 study. Factor 6 is identified as oil combustion because of the high levels of V and Ni

377 (Moreno et al., 2011; Minguillón et al., 2014; Huang et al., 2018).

378 The source contributions of DTT<sub>v</sub> in the south and north of Beijing are shown in  
379 Figure 5, exhibiting obvious district differences. In the south, traffic-related emissions  
380 (39.1%) and biomass burning (25.2%) had the most contribution to DTT<sub>v</sub>, followed  
381 by secondary formation (17.2%), coal burning (15%), dust (2%), and oil combustion  
382 (1.5%). In the north, traffic-related emissions (51.6%) had the highest contribution to  
383 DTT<sub>v</sub>, followed by coal burning (19.9%), secondary formation (13%), biomass  
384 burning (8.4%), oil combustion (4.1%), and dust (3%). The large district differences  
385 in sources of DTT<sub>v</sub> of water-soluble PM<sub>2.5</sub> call for more research on the relationship  
386 between sources, chemical composition, formation processes and OP of PM<sub>2.5</sub>.

387

#### 388 **4 Conclusions**

389 In this study, the water-soluble OP of ambient PM<sub>2.5</sub> collected in winter in the  
390 south and north of Beijing were quantified, together with the concentration and light  
391 absorption of WSOC, and concentrations of 7 light-absorbing NACs and 14 trace  
392 elements. The average DTT<sub>v</sub> value was comparable in the south ( $3.9 \pm 0.9 \text{ nmol min}^{-1}$   
393  $\text{m}^{-3}$ ) and north ( $3.5 \pm 1.2 \text{ nmol min}^{-1} \text{ m}^{-3}$ ), while the DTT<sub>m</sub> was higher in the north  
394 ( $65.3 \pm 27.6 \text{ pmol min}^{-1} \mu\text{g}^{-1}$ ) than in the south ( $36.1 \pm 14.5 \text{ pmol min}^{-1} \mu\text{g}^{-1}$ ),  
395 indicating that the exposure-relevant OP of water-soluble components of PM<sub>2.5</sub> was  
396 similar in the two sites and that the intrinsic OP of water-soluble components of PM<sub>2.5</sub>  
397 was higher in the north than in the south. The correlation between DTT<sub>v</sub> and soluble  
398 elements was higher than that between DTT<sub>v</sub> and total elements in both the south and  
399 north. In the north, the DTT<sub>v</sub> was strongly correlated with soluble Mn, Co, Ni, Zn, As,  
400 Cd and Pb ( $r > 0.7$ ), and in the south it positively correlated with Mn, Fe, Cr, Co, As  
401 and Pb ( $r > 0.5$ ). In addition, in the north the DTT<sub>v</sub> was also positively correlated with  
402 WSOC, Abs<sub>365</sub> and NACs ( $r$  of 0.56 to 0.79), while in the south it was weakly  
403 correlated ( $r \leq 0.4$ ). These results indicate that in the north trace elements and water-  
404 soluble organic compounds, especially BrC chromophores, both had significant  
405 contributions to DTT consumption, and in the south the consumption of DTT may be

406 mainly from trace elements. Six sources of  $DTT_v$  were resolved with the PMF model,  
407 including biomass burning, coal burning, traffic-related, dust, oil combustion, and  
408 secondary formation. On average, traffic-related emissions (39.1%) and biomass  
409 burning (25.2%) were the major contributors of  $DTT_v$  in the south, and traffic-related  
410 emissions (51.6%) was the predominated source in the north. The differences in  $DTT_v$   
411 sources in the south and north of Beijing suggest that the relationship between source  
412 emissions and atmospheric processes and  $PM_{2.5}$  OP deserve further exploration in  
413 order to better understand the regional differences of health impacts of  $PM_{2.5}$ .

414

415

416

417 **Date availability.** Raw data used in this study can be obtained from the following  
418 open link: <https://doi.org/10.5281/zenodo.10791126> (Yuan et al., 2024). It is also  
419 available on request by contacting the corresponding author.

420

421 **Supplement.** The Supplement related to this article is available online.

422

423 **Author contributions.** RJH designed the study. Data analysis was done by WY, CL,  
424 LY, HY and RJH. WY, CL, LY, HY and RJH interpreted data, prepared the display  
425 items and wrote the manuscript. All authors commented on and discussed the  
426 manuscript.

427

428 **Competing interests.** The authors declare that they have no conflict of interest.

429

430 **Acknowledgements.** We are very grateful to the National Natural Science Foundation  
431 of China (NSFC) under Grant No. 41925015, the Strategic Priority Research Program  
432 of Chinese Academy of Sciences (XDB40000000), the Key Research Program of  
433 Frontier Sciences from the Chinese Academy of Sciences (ZDBS-LY-DQC001), the  
434 New Cornerstone Science Foundation through the XPLOER PRIZE, and the

435 Postdoctoral Fellowship Program of CPSF (no. GZC20232628) supported this study.

436

437 **Financial support.** This work was supported by the National Natural Science  
438 Foundation of China (NSFC) under Grant No. 41925015, the Strategic Priority  
439 Research Program of Chinese Academy of Sciences (XDB40000000), the Key  
440 Research Program of Frontier Sciences from the Chinese Academy of Sciences  
441 (ZDBS-LY-DQC001), the New Cornerstone Science Foundation through the  
442 XPLOER PRIZE, and the Postdoctoral Fellowship Program of CPSF (no.  
443 GZC20232628).

444

445

#### 446 **References**

447 Ahmad, M., Yu, Q., Chen, J., Cheng, S., Qin, W., and Zhang, Y.: Chemical  
448 characteristics, oxidative potential, and sources of PM<sub>2.5</sub> in wintertime in  
449 Lahore and Peshawar, Pakistan, *J. Environ. Sci.*, 102, 148-158,  
450 10.1016/j.jes.2020.09.014, 2021.

451 Al-Naiema, I. M. and Stone, E. A.: Evaluation of anthropogenic secondary organic  
452 aerosol tracers from aromatic hydrocarbons, *Atmos. Chem. Phys.*, 17, 2053-  
453 2065, 10.5194/acp-17-2053-2017, 2017.

454 An, Z., Huang, R. J., Zhang, R., Tie, X., Li, G., Cao, J., Zhou, W., Shi, Z., Han, Y., Gu,  
455 Z., and Ji, Y.: Severe haze in northern China: A synergy of anthropogenic  
456 emissions and atmospheric processes, *Proc. Natl. Acad. Sci. U. S. A.*, 116,  
457 8657-8666, 10.1073/pnas.1900125116, 2019.

458 Bates, J. T., Fang, T., Verma, V., Zeng, L., Weber, R. J., Tolbert, P. E., Abrams, J. Y.,  
459 Sarnat, S. E., Klein, M., Mulholland, J. A., and Russell, A. G.: Review of  
460 Acellular Assays of Ambient Particulate Matter Oxidative Potential: Methods  
461 and Relationships with Composition, Sources, and Health Effects, *Environ.*  
462 *Sci. Technol.*, 53, 4003-4019, 10.1021/acs.est.8b03430, 2019.

463 Belis, C., Larsen, B. R., Amato, F., Haddad, I. El, Favez, O., Harrison, R. M., Hopke,



464 P. K., Nava, S., Paatero, P., Prévôt, A., Quass, U., Vecchi, R., and Viana, M.:  
465 European Guide on Air Pollution Source Apportionment with Receptor  
466 Models, JRC References Report, March, 88, 1-170,  
467 <https://doi.org/10.2788/9307>, 2019.

468 Burnett, R., Chen, H., Szyszkowicz, M., Fann, N., Hubbell, B., Pope, C. A., 3rd, Apte,  
469 J. S., Brauer, M., Cohen, A., Weichenthal, S., Coggins, J., Di, Q., Brunekreef,  
470 B., Frostad, J., Lim, S. S., Kan, H., Walker, K. D., Thurston, G. D., Hayes, R.  
471 B., Lim, C. C., Turner, M. C., Jerrett, M., Krewski, D., Gapstur, S. M., Diver,  
472 W. R., Ostro, B., Goldberg, D., Crouse, D. L., Martin, R. V., Peters, P., Pinault,  
473 L., Tjepkema, M., van Donkelaar, A., Villeneuve, P. J., Miller, A. B., Yin, P.,  
474 Zhou, M., Wang, L., Janssen, N. A. H., Marra, M., Atkinson, R. W., Tsang, H.,  
475 Quoc Thach, T., Cannon, J. B., Allen, R. T., Hart, J. E., Laden, F., Cesaroni, G.,  
476 Forastiere, F., Weinmayr, G., Jaensch, A., Nagel, G., Concin, H., and Spadaro,  
477 J. V.: Global estimates of mortality associated with long-term exposure to  
478 outdoor fine particulate matter, *Proc. Natl. Acad. Sci. U. S. A.*, 115, 9592-9597,  
479 [10.1073/pnas.1803222115](https://doi.org/10.1073/pnas.1803222115), 2018.

480 Calas, A., Uzu, G., Kelly, F. J., Houdier, S., Martins, J. M. F., Thomas, F., Molton, F.,  
481 Charron, A., Dunster, C., Oliete, A., Jacob, V., Besombes, J.-L., Chevrier, F.,  
482 and Jaffrezo, J.-L.: Comparison between five acellular oxidative potential  
483 measurement assays performed with detailed chemistry on PM<sub>10</sub> samples from  
484 the city of Chamonix (France), *Atmos. Chem. Phys.*, 18, 7863-7875,  
485 [10.5194/acp-18-7863-2018](https://doi.org/10.5194/acp-18-7863-2018), 2018.

486 Campbell, S. J., Wolfer, K., Utinger, B., Westwood, J., Zhang, Z. H., Bukowiecki, N.,  
487 Steimer, S. S., Vu, T. V., Xu, J., Straw, N., Thomson, S., Elzein, A., Sun, Y.,  
488 Liu, D., Li, L., Fu, P., Lewis, A. C., Harrison, R. M., Bloss, W. J., Loh, M.,  
489 Miller, M. R., Shi, Z., and Kalberer, M.: Atmospheric conditions and  
490 composition that influence PM<sub>2.5</sub> oxidative potential in Beijing, China, *Atmos.*  
491 *Chem. Phys.*, 21, 5549-5573, [10.5194/acp-21-5549-2021](https://doi.org/10.5194/acp-21-5549-2021), 2021.

492 Cao, T., Li, M., Zou, C., Fan, X., Song, J., Jia, W., Yu, C., Yu, Z., and Peng, P. a.:

493 Chemical composition, optical properties, and oxidative potential of water-  
494 and methanol-soluble organic compounds emitted from the combustion of  
495 biomass materials and coal, *Atmos. Chem. Phys.*, 21, 13187-13205,  
496 10.5194/acp-21-13187-2021, 2021.

497 Charrier, J. G. and Anastasio, C.: On dithiothreitol (DTT) as a measure of oxidative  
498 potential for ambient particles: evidence for the importance of soluble  
499 transition metals, *Atmos. Chem. Phys.*, 12, 9321-9333, 10.5194/acp-12-9321-  
500 2012, 2012.

501 Charrier, J. G., McFall, A. S., Vu, K. K.-T., Baroi, J., Olea, C., Hasson, A., and  
502 Anastasio, C.: A Bias in the “Mass-Normalized” DTT Response-An Effect of  
503 Non-Linear Concentration Response Curves for Copper and Manganese,  
504 *Atmos. Environ.*, 144, 325-334, 2016.

505 Chen, K., Xu, J., Famiyeh, L., Sun, Y., Ji, D., Xu, H., Wang, C., Metcalfe, S. E., Betha,  
506 R., Behera, S. N., Jia, C., Xiao, H., and He, J.: Chemical constituents, driving  
507 factors, and source apportionment of oxidative potential of ambient fine  
508 particulate matter in a Port City in East China, *J. Hazard. Mater.*, 440,  
509 10.1016/j.jhazmat.2022.129864, 2022.

510 Chen, Q., Wang, M., Wang, Y., Zhang, L., Li, Y., and Han, Y.: Oxidative Potential of  
511 Water-Soluble Matter Associated with Chromophoric Substances in PM<sub>2.5</sub> over  
512 Xi'an, China, *Environ. Sci. Technol.*, 53, 8574-8584, 10.1021/acs.est.9b01976,  
513 2019.

514 Chirizzi, D., Cesari, D., Guascito, M. R., Dinoi, A., Giotta, L., Donateo, A., and  
515 Contini, D.: Influence of Saharan dust outbreaks and carbon content on  
516 oxidative potential of water-soluble fractions of PM<sub>2.5</sub> and PM<sub>10</sub>, *Atmos.*  
517 *Environ.*, 163, 1-8, 10.1016/j.atmosenv.2017.05.021, 2017.

518 Chow, W. S., Huang, X. H. H., Leung, K. F., Huang, L., Wu, X., and Yu, J. Z.:  
519 Molecular and elemental marker-based source apportionment of fine  
520 particulate matter at six sites in Hong Kong, China, *Sci. Total Environ.*, 813,  
521 152652, 10.1016/j.scitotenv.2021.152652, 2022.

522 Chowdhury, P. H., He, Q., Carmieli, R., Li, C., Rudich, Y., and Pardo, M.: Connecting  
523 the Oxidative Potential of Secondary Organic Aerosols with Reactive Oxygen  
524 Species in Exposed Lung Cells, *Environ. Sci. Technol.*, 53, 13949-13958,  
525 10.1021/acs.est.9b04449, 2019.

526 Cui, Y., Zhu, L., Wang, H., Zhao, Z., Ma, S., and Ye, Z.: Characteristics and Oxidative  
527 Potential of Ambient PM<sub>2.5</sub> in the Yangtze River Delta Region: Pollution Level  
528 and Source Apportionment, *Atmosphere*, 14, 10.3390/atmos14030425, 2023.

529 Daellenbach, K. R., Uzu, G., Jiang, J., Cassagnes, L. E., Leni, Z., Vlachou, A.,  
530 Stefanelli, G., Canonaco, F., Weber, S., Segers, A., Kuenen, J. J. P., Schaap, M.,  
531 Favez, O., Albinet, A., Aksoyoglu, S., Dommen, J., Baltensperger, U., Geiser,  
532 M., El Haddad, I., Jaffrezo, J. L., and Prevot, A. S. H.: Sources of particulate-  
533 matter air pollution and its oxidative potential in Europe, *Nature*, 587, 414-419,  
534 10.1038/s41586-020-2902-8, 2020.

535 Fan, X., Li, M., Cao, T., Cheng, C., Li, F., Xie, Y., Wei, S., Song, J., and Peng, P. a.:  
536 Optical properties and oxidative potential of water- and alkaline-soluble  
537 brown carbon in smoke particles emitted from laboratory simulated biomass  
538 burning, *Atmos. Environ.*, 194, 48-57, 10.1016/j.atmosenv.2018.09.025, 2018.

539 Fang, T., Verma, V., Bates, J. T., Abrams, J., Klein, M., Strickland, M. J., Sarnat, S. E.,  
540 Chang, H. H., Mulholland, J. A., Tolbert, P. E., Russell, A. G., and Weber, R. J.:  
541 Oxidative potential of ambient water-soluble PM<sub>2.5</sub> in the southeastern United  
542 States: contrasts in sources and health associations between ascorbic acid (AA)  
543 and dithiothreitol (DTT) assays, *Atmos. Chem. Phys.*, 16, 3865-3879,  
544 10.5194/acp-16-3865-2016, 2016.

545 Feng, R., Xu, H., Gu, Y., Wang, Z., Han, B., Sun, J., Liu, S., Lu, H., Ho, S. S. H.,  
546 Shen, Z., and Cao, J.: Variations of Personal Exposure to Particulate Nitrated  
547 Phenols from Heating Energy Renovation in China: The First Assessment on  
548 Associated Toxicological Impacts with Particle Size Distributions, *Environ.*  
549 *Sci. Technol.*, 56, 3974-3983, 2022.

550 Gao, D., Fang, T., Verma, V., Zeng, L., and Weber, R. J.: A method for measuring total

551 aerosol oxidative potential (OP) with the dithiothreitol (DTT) assay and  
552 comparisons between an urban and roadside site of water-soluble and total OP,  
553 *Atmos. Meas. Tech.*, 10, 2821-2835, 10.5194/amt-10-2821-2017, 2017.

554 Hecobian, A., Zhang, X., Zheng, M., Frank, N., Edgerton, E. S., and Weber, R. J.:  
555 Water-Soluble Organic Aerosol material and the light-absorption  
556 characteristics of aqueous extracts measured over the Southeastern United  
557 States, *Atmos. Chem. Phys.*, 10, 5965-5977, 10.5194/acp-10-5965-2010, 2010.

558 Ho, K. F., Ho, S. S. H., Huang, R.-J., Liu, S. X., Cao, J.-J., Zhang, T., Chuang, H.-C.,  
559 Chan, C. S., Hu, D., and Tian, L.: Characteristics of water-soluble organic  
560 nitrogen in fine particulate matter in the continental area of China, *Atmos.*  
561 *Environ.*, 106, 252-261, 10.1016/j.atmosenv.2015.02.010, 2015.

562 Huang, R. J., Cheng, R., Jing, M., Yang, L., Li, Y., Chen, Q., Chen, Y., Yan, J., Lin, C.,  
563 Wu, Y., Zhang, R., El Haddad, I., Prevot, A. S. H., O'Dowd, C. D., and Cao, J.:  
564 Source-Specific Health Risk Analysis on Particulate Trace Elements: Coal  
565 Combustion and Traffic Emission As Major Contributors in Wintertime  
566 Beijing, *Environ. Sci. Technol.*, 52, 10967-10974, 10.1021/acs.est.8b02091,  
567 2018.

568 Huang, R. J., Yang, L., Shen, J., Yuan, W., Gong, Y., Guo, J., Cao, W., Duan, J., Ni, H.,  
569 Zhu, C., Dai, W., Li, Y., Chen, Y., Chen, Q., Wu, Y., Zhang, R., Dusek, U.,  
570 O'Dowd, C., and Hoffmann, T.: Water-Insoluble Organics Dominate Brown  
571 Carbon in Wintertime Urban Aerosol of China: Chemical Characteristics and  
572 Optical Properties, *Environ. Sci. Technol.*, 54, 7836-7847,  
573 10.1021/acs.est.0c01149, 2020.

574 Huang, R. J., Zhang, Y., Bozzetti, C., Ho, K. F., Cao, J. J., Han, Y., Daellenbach, K. R.,  
575 Slowik, J. G., Platt, S. M., Canonaco, F., Zotter, P., Wolf, R., Pieber, S. M.,  
576 Bruns, E. A., Crippa, M., Ciarelli, G., Piazzalunga, A., Schwikowski, M.,  
577 Abbaszade, G., Schnelle-Kreis, J., Zimmermann, R., An, Z., Szidat, S.,  
578 Baltensperger, U., El Haddad, I., and Prevot, A. S.: High secondary aerosol  
579 contribution to particulate pollution during haze events in China, *Nature*, 514,

580 218-222, 10.1038/nature13774, 2014.

581 Jiang, H., Xie, Y., Ge, Y., He, H., and Liu, Y.: Effects of ultrasonic treatment on  
582 dithiothreitol (DTT) assay measurements for carbon materials, *J. Environ. Sci.*,  
583 84, 51–58, 2019.

584 Joo, H. S., Batmunkh, T., Borlaza, L. J. S., Park, M., Lee, K. Y., Lee, J. Y., Chang, Y.  
585 W., and Park, K.: Physicochemical properties and oxidative potential of fine  
586 particles produced from coal combustion, *Aerosol Sci. Technol.*, 52, 1134-  
587 1144, 10.1080/02786826.2018.1501152, 2018.

588 Khoshnamvand, N., Nodehi, R. N., Hassanvand, M. S., and Naddafi, K.: Comparison  
589 between oxidative potentials measured of water-soluble components in  
590 ambient air PM<sub>1</sub> and PM<sub>2.5</sub> of Tehran, Iran, *Air Qual. Atmos. Hlth.*, 16, 1311-  
591 1320, 10.1007/s11869-023-01343-y, 2023.

592 Laskin, A., Laskin, J., and Nizkorodov, S. A.: Chemistry of atmospheric brown carbon,  
593 *Chem. Rev.*, 115, 4335-4382, 10.1021/cr5006167, 2015.

594 Lelieveld, S., Wilson, J., Dovrou, E., Mishra, A., Lakey, P. S. J., Shiraiwa, M., Poschl,  
595 U., and Berkemeier, T.: Hydroxyl Radical Production by Air Pollutants in  
596 Epithelial Lining Fluid Governed by Interconversion and Scavenging of  
597 Reactive Oxygen Species, *Environ. Sci. Technol.*, 55, 14069-14079,  
598 10.1021/acs.est.1c03875, 2021.

599 Lin, P., Bluvshstein, N., Rudich, Y., Nizkorodov, S. A., Laskin, J., and Laskin, A.:  
600 Molecular chemistry of atmospheric brown carbon inferred from a nationwide  
601 biomass burning event, *Environ. Sci. Technol.*, 51, 11561–11570, 2017.

602 Liu, W., Xu, Y., Liu, W., Liu, Q., Yu, S., Liu, Y., Wang, X., and Tao, S.: Oxidative  
603 potential of ambient PM<sub>2.5</sub> in the coastal cities of the Bohai Sea, northern  
604 China: Seasonal variation and source apportionment, *Environ. Pollut.*, 236,  
605 514-528, 10.1016/j.envpol.2018.01.116, 2018.

606 Liu, Y., Yan, C. Q., Ding, X., Wang, X. M., Fu, Q. Y., Zhao, Q. B., Zhang, Y. H., Duan,  
607 Y. S., Qiu, X. H., and Zheng, M.: Sources and spatial distribution of  
608 particulate polycyclic aromatic hydrocarbons in Shanghai, China, *Sci. Total*

609 Environ., 584-585, 307-317, <https://doi.org/10.1016/j.scitotenv.2016.12.134>,  
610 2017.

611 Ma, X., Nie, D., Chen, M., Ge, P., Liu, Z., Ge, X., Li, Z., and Gu, R.: The Relative  
612 Contributions of Different Chemical Components to the Oxidative Potential of  
613 Ambient Fine Particles in Nanjing Area, *Int. J. Environ. Res. Public Health*, 18,  
614 2789, 10.3390/ijerph18062789, 2021.

615 Miljevic, B., Hedayat, F., Stevanovic, S., Fairfull-Smith, K. E., Bottle, S. E., and  
616 Ristovski, Z. D.: To sonicate or not to sonicate PM filters: reactive oxygen  
617 species generation upon ultrasonic irradiation, *Aerosol. Sci. Technol.*, 48,  
618 1276-1284, 2014.

619 Minguillón, M. C., Cirach, M., Hoek, G., Brunekreef, B., Tsai, M., de Hoogh, K.,  
620 Jedynska, A., Kooter, I. M., Nieuwenhuijsen, M., and Querol, X.: Spatial  
621 variability of trace elements and sources for improved exposure assessment in  
622 Barcelona, *Atmos. Environ.*, 89, 268-281, 10.1016/j.atmosenv.2014.02.047,  
623 2014.

624 Moreno, T., Querol, X., Alastuey, A., Reche, C., Cusack, M., Amato, F., Pandolfi, M.,  
625 Pey, J., Richard, A., Prévôt, A. S. H., Furger, M., and Gibbons, W.: Variations  
626 in time and space of trace metal aerosol concentrations in urban areas and their  
627 surroundings, *Atmos. Chem. Phys.*, 11, 9415-9430, 10.5194/acp-11-9415-2011,  
628 2011.

629 Oh, S. H., Park, K., Park, M., Song, M., Jang, K. S., Schauer, J. J., Bae, G. N., and  
630 Bae, M. S.: Comparison of the sources and oxidative potential of PM<sub>2.5</sub> during  
631 winter time in large cities in China and South Korea, *Sci. Total Environ.*, 859,  
632 160369, 10.1016/j.scitotenv.2022.160369, 2023.

633 Paatero, P.: Least squares formation of robust non negative factor analysis,  
634 *Chemometr. Intell. Lab.*, 37, 23-35, 1997.

635 Puthussery, J. V., Dave, J., Shukla, A., Gaddamidi, S., Singh, A., Vats, P., Salana, S.,  
636 Ganguly, D., Rastogi, N., Tripathi, S. N., and Verma, V.: Effect of Biomass  
637 Burning, Diwali Fireworks, and Polluted Fog Events on the Oxidative

638 Potential of Fine Ambient Particulate Matter in Delhi, India, *Environ. Sci.*  
639 *Technol.*, 56, 14605-14616, 10.1021/acs.est.2c02730, 2022.

640 Shen, J., Taghvaei, S., La, C., Oroumijeh, F., Liu, J., Jerrett, M., Weichenthal, S., Del  
641 Rosario, I., Shafer, M. M., Ritz, B., Zhu, Y., and Paulson, S. E.: Aerosol  
642 Oxidative Potential in the Greater Los Angeles Area: Source Apportionment  
643 and Associations with Socioeconomic Position, *Environ. Sci. Technol.*, 56,  
644 17795-17804, 10.1021/acs.est.2c02788, 2022.

645 Ting, Y. C., Chang, P. K., Hung, P. C., Chou, C. C., Chi, K. H., and Hsiao, T. C.:  
646 Characterizing emission factors and oxidative potential of motorcycle  
647 emissions in a real-world tunnel environment, *Environ. Res.*, 234, 116601,  
648 10.1016/j.envres.2023.116601, 2023.

649 Tong, H., Lakey, P. S. J., Arangio, A. M., Socorro, J., Kampf, C. J., Berkemeier, T.,  
650 Brune, W. H., Poschl, U., and Shiraiwa, M.: Reactive oxygen species formed  
651 in aqueous mixtures of secondary organic aerosols and mineral dust  
652 influencing cloud chemistry and public health in the Anthropocene, *Faraday*  
653 *Discuss.*, 200, 251-270, 10.1039/c7fd00023e, 2017.

654 Tong, H., Lakey, P. S. J., Arangio, A. M., Socorro, J., Shen, F., Lucas, K., Brune, W.  
655 H., Poschl, U., and Shiraiwa, M.: Reactive Oxygen Species Formed by  
656 Secondary Organic Aerosols in Water and Surrogate Lung Fluid, *Environ. Sci.*  
657 *Technol.*, 52, 11642-11651, 10.1021/acs.est.8b03695, 2018.

658 Tuet, W. Y., Chen, Y., Xu, L., Fok, S., Gao, D., Weber, R. J., and Ng, N. L.: Chemical  
659 oxidative potential of secondary organic aerosol (SOA) generated from the  
660 photooxidation of biogenic and anthropogenic volatile organic compounds,  
661 *Atmos. Chem. Phys.*, 17, 839-853, 10.5194/acp-17-839-2017, 2017.

662 Tuet, W. Y., Liu, F., de Oliveira Alves, N., Fok, S., Artaxo, P., Vasconcellos, P.,  
663 Champion, J. A., and Ng, N. L.: Chemical Oxidative Potential and Cellular  
664 Oxidative Stress from Open Biomass Burning Aerosol, *Environ. Sci. Technol.*  
665 *Lett.*, 6, 126-132, 10.1021/acs.estlett.9b00060, 2019.

666 Verma, V., Fang, T., Xu, L., Peltier, R. E., Russell, A. G., Ng, N. L., and Weber, R. J.:

667 Organic aerosols associated with the generation of reactive oxygen species  
668 (ROS) by water-soluble PM<sub>2.5</sub>, *Environ. Sci. Technol.*, 49, 4646-4656,  
669 10.1021/es505577w, 2015.

670 Verma, V., Rico-Martinez, R., Kotra, N., King, L., Liu, J., Snell, T. W., and Weber, R.  
671 J.: Contribution of water-soluble and insoluble components and their  
672 hydrophobic/hydrophilic subfractions to the reactive oxygen species-  
673 generating potential of fine ambient aerosols, *Environ. Sci. Technol.*, 46,  
674 11384-11392, 10.1021/es302484r, 2012.

675 Verma, V., Fang, T., Guo, H., King, L., Bates, J. T., Peltier, R. E., Edgerton, E.,  
676 Russell, A. G., and Weber, R. J.: Reactive oxygen species associated with  
677 water-soluble PM<sub>2.5</sub> in the southeastern United States: spatiotemporal trends  
678 and source apportionment, *Atmos. Chem. Phys.*, 14, 12915-12930,  
679 10.5194/acp-14-12915-2014, 2014.

680 Vreeland, H., Weber, R., Bergin, M., Greenwald, R., Golan, R., Russell, A. G., Verma,  
681 V., and Sarnat, J. A.: Oxidative potential of PM<sub>2.5</sub> during Atlanta rush hour:  
682 Measurements of in-vehicle dithiothreitol (DTT) activity, *Atmos. Environ.*,  
683 165, 169-178, 10.1016/j.atmosenv.2017.06.044, 2017.

684 Wang, J., Lin, X., Lu, L., Wu, Y., Zhang, H., Lv, Q., Liu, W., Zhang, Y., and Zhuang,  
685 S.: Temporal variation of oxidative potential of water soluble components of  
686 ambient PM<sub>2.5</sub> measured by dithiothreitol (DTT) assay, *Sci. Total Environ.*,  
687 649, 969-978, 10.1016/j.scitotenv.2018.08.375, 2019.

688 Wang, T., Huang, R. J., Li, Y., Chen, Q., Chen, Y., Yang, L., Guo, J., Ni, H., Hoffmann,  
689 T., Wang, X., and Mai, B.: One-year characterization of organic aerosol  
690 markers in urban Beijing: Seasonal variation and spatiotemporal comparison,  
691 *Sci. Total Environ.*, 743, 140689, 10.1016/j.scitotenv.2020.140689, 2020a.

692 Wang, Y., Wang, M., Li, S., Sun, H., Mu, Z., Zhang, L., Li, Y., and Chen, Q.: Study on  
693 the oxidation potential of the water-soluble components of ambient PM<sub>2.5</sub> over  
694 Xi'an, China: Pollution levels, source apportionment and transport pathways,  
695 *Environ. Int.*, 136, 105515, 10.1016/j.envint.2020.105515, 2020b.



696 Wong, J. P. S., Tsagkaraki, M., Tsiodra, I., Mihalopoulos, N., Violaki, K., Kanakidou,  
697 M., Sciare, J., Nenes, A., and Weber, R. J.: Effects of Atmospheric Processing  
698 on the Oxidative Potential of Biomass Burning Organic Aerosols, *Environ. Sci.*  
699 *Technol.*, 53, 6747-6756, 10.1021/acs.est.9b01034, 2019.

700 Wu, N., Lu, B., Chen, Q., Chen, J., and Li, X.: Connecting the Oxidative Potential of  
701 Fractionated Particulate Matter With Chromophoric Substances, *J. Geophys.*  
702 *Res-Atmos.*, 127, 10.1029/2021jd035503, 2022a.

703 Wu, N., Lyu, Y., Lu, B., Cai, D., Meng, X., and Li, X.: Oxidative potential induced by  
704 metal-organic interaction from PM<sub>2.5</sub> in simulated biological fluids, *Sci. Total*  
705 *Environ.*, 848, 157768, 10.1016/j.scitotenv.2022.157768, 2022b.

706 Xing, C., Wang, Y., Yang, X., Zeng, Y., Zhai, J., Cai, B., Zhang, A., Fu, T. M., Zhu, L.,  
707 Li, Y., Wang, X., and Zhang, Y.: Seasonal variation of driving factors of  
708 ambient PM<sub>2.5</sub> oxidative potential in Shenzhen, China, *Sci. Total Environ.*, 862,  
709 160771, 10.1016/j.scitotenv.2022.160771, 2023.

710 Xiong, Q., Yu, H., Wang, R., Wei, J., and Verma, V.: Rethinking Dithiothreitol-Based  
711 Particulate Matter Oxidative Potential: Measuring Dithiothreitol Consumption  
712 versus Reactive Oxygen Species Generation, *Environ. Sci. Technol.*, 51, 6507-  
713 6514, 10.1021/acs.est.7b01272, 2017.

714 Yalamanchili, J., Hennigan, C. J., and Reed, B. E.: Measurement artifacts in the  
715 dithiothreitol (DTT) oxidative potential assay caused by interactions between  
716 aqueous metals and phosphate buffer, *J. Hazard. Mater.*, 456, 131693, 2023.

717 Yu, H., Wei, J., Cheng, Y., Subedi, K., and Verma, V.: Synergistic and Antagonistic  
718 Interactions among the Particulate Matter Components in Generating Reactive  
719 Oxygen Species Based on the Dithiothreitol Assay, *Environ. Sci. Technol.*, 52,  
720 2261–2270, 2018.

721 Yu, Q., Chen, J., Qin, W., Ahmad, M., Zhang, Y., Sun, Y., Xin, K., and Ai, J.:  
722 Oxidative potential associated with water-soluble components of PM<sub>2.5</sub> in  
723 Beijing: The important role of anthropogenic organic aerosols, *J. Hazard.*  
724 *Mater.*, 433, 128839, 10.1016/j.jhazmat.2022.128839, 2022a.

725 Yu, S., Liu, W., Xu, Y., Yi, K., Zhou, M., Tao, S., and Liu, W.: Characteristics and  
726 oxidative potential of atmospheric PM<sub>2.5</sub> in Beijing: Source apportionment and  
727 seasonal variation, *Sci. Total Environ.*, 650, 277-287,  
728 10.1016/j.scitotenv.2018.09.021, 2019.

729 Yu, Y., Sun, Q., Li, T., Ren, X., Lin, L., Sun, M., Duan, J., and Sun, Z.: Adverse  
730 outcome pathway of fine particulate matter leading to increased cardiovascular  
731 morbidity and mortality: An integrated perspective from toxicology and  
732 epidemiology, *J. Hazard. Mater.*, 430, 128368, 10.1016/j.jhazmat.2022.128368,  
733 2022b.

734 Yu, Y., Cheng, P., Li, Y., Gu, J., Gong, Y., Han, B., Yang, W., Sun, J., Wu, C., Song,  
735 W., and Li, M.: The association of chemical composition particularly the  
736 heavy metals with the oxidative potential of ambient PM<sub>2.5</sub> in a megacity  
737 (Guangzhou) of southern China, *Environ. Res.*, 213, 113489,  
738 10.1016/j.envres.2022.113489, 2022c.

739 Yuan, W., Huang, R.-J., Luo, C., Yang, L., Cao, W., Guo, J., and Yang, H.:  
740 Measurement report: Oxidation potential of water-soluble aerosol components  
741 in the southern and northern of Beijing, Zenodo [data set],  
742 <https://doi.org/10.5281/zenodo.10791126>, 2024.

743 Yuan, W., Huang, R.-J., Yang, L., Guo, J., Chen, Z., Duan, J., Wang, T., Ni, H., Han,  
744 Y., Li, Y., Chen, Q., Chen, Y., Hoffmann, T., and O'Dowd, C.: Characterization  
745 of the light-absorbing properties, chromophore composition and sources of  
746 brown carbon aerosol in Xi'an, northwestern China, *Atmos. Chem. Phys.*, 20,  
747 5129-5144, 10.5194/acp-20-5129-2020, 2020.

748 Zhang, Q., Ma, H., Li, J., Jiang, H., Chen, W., Wan, C., Jiang, B., Dong, G., Zeng, X.,  
749 Chen, D., Lu, S., You, J., Yu, Z., Wang, X., and Zhang, G.: Nitroaromatic  
750 Compounds from Secondary Nitrate Formation and Biomass Burning Are  
751 Major Proinflammatory Components in Organic Aerosols in Guangzhou: A  
752 Bioassay Combining High-Resolution Mass Spectrometry Analysis, *Environ.*  
753 *Sci. Technol.*, 57, 21570-21580, <https://doi.org/10.1021/acs.est.3c04983>, 2023.

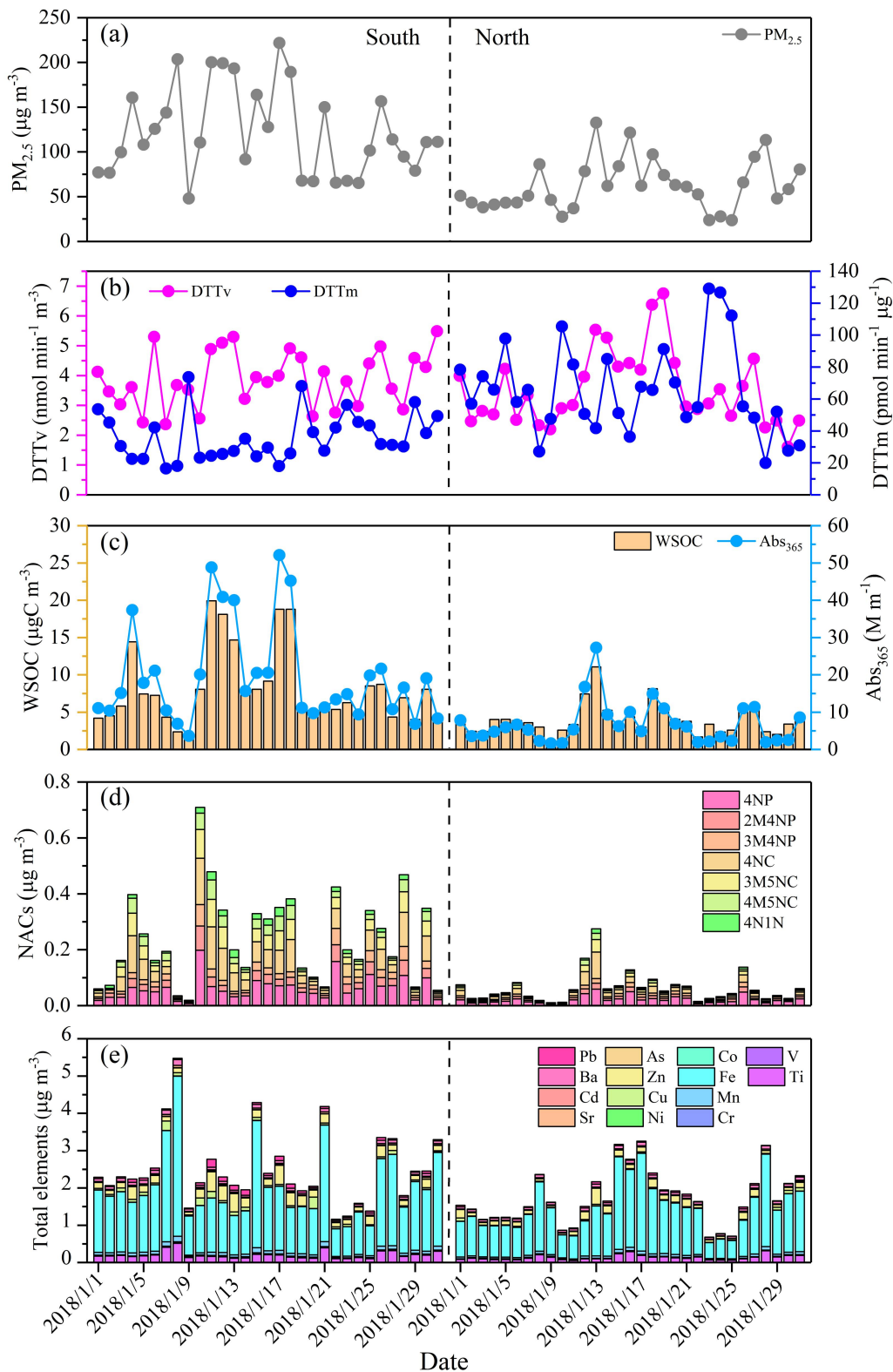
754 Zheng, Y., Davis, S. J., Persad, G. G., and Caldeira, K.: Climate effects of aerosols  
755 reduce economic inequality, *Nat. Clim. Chang.*, 10, 220-224, 2020.

756

757

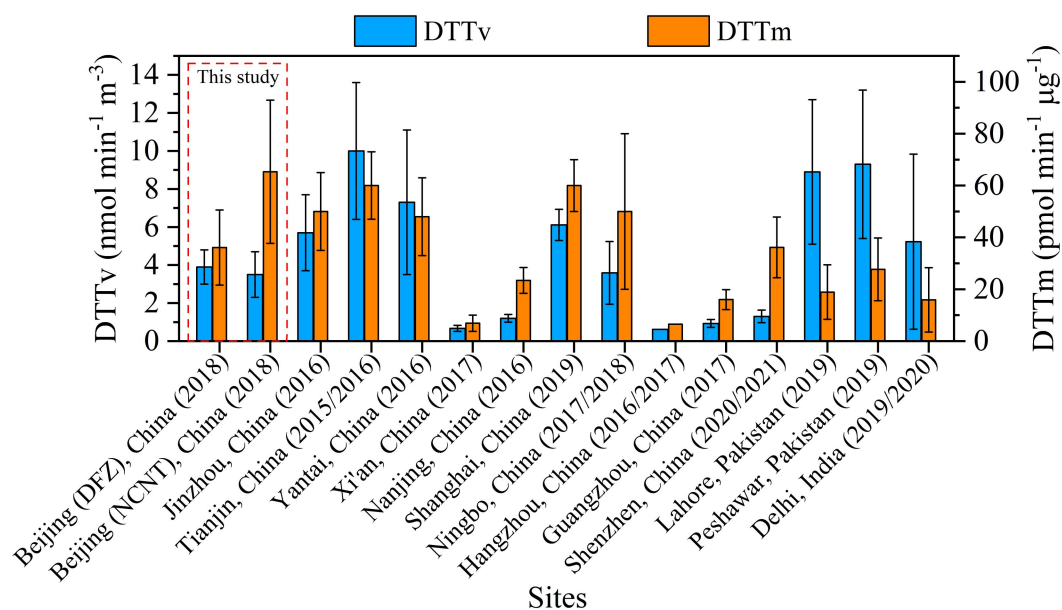
758

759



760

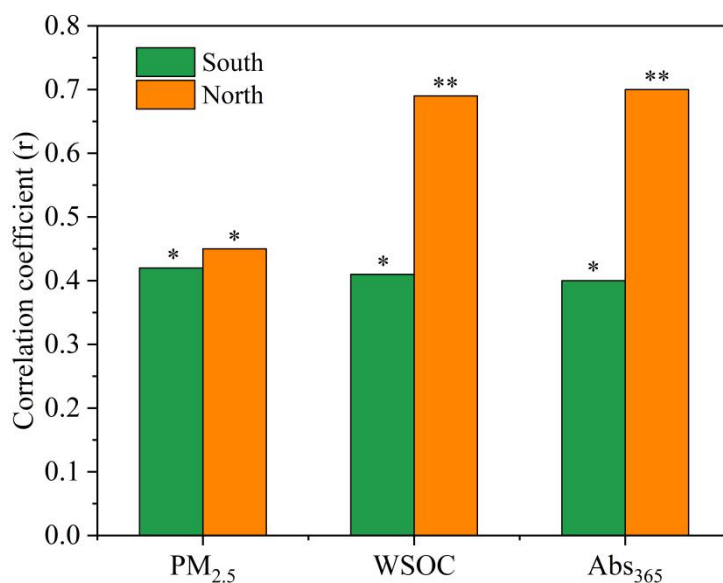
761 **Figure 1.** Time series of (a) PM<sub>2.5</sub> concentration, (b) DTT<sub>v</sub> and DTT<sub>m</sub>, (c)  
 762 concentration and light absorption at wavelength 365 nm (Abs<sub>365</sub>) of WSOC,  
 763 concentrations of (d) NACs and (e) elements.



764

765 **Figure 2.** Comparison of DTT<sub>v</sub> and DTT<sub>m</sub> values of water-soluble PM<sub>2.5</sub> measured in  
 766 this study with those measured in other areas of Asia during similar period.

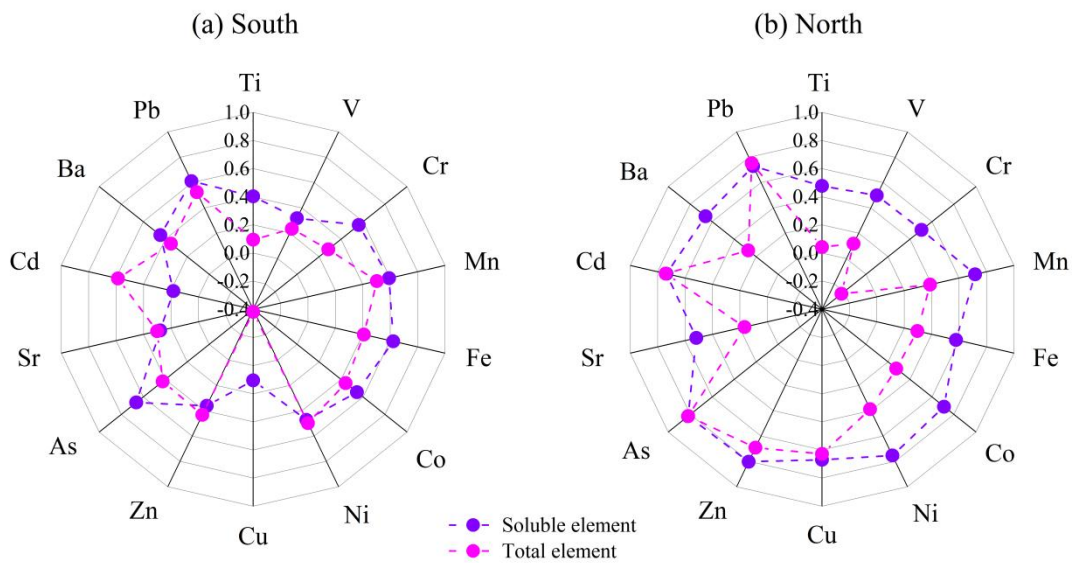
767



768

769 **Figure 3.** Correlation coefficients between DTT<sub>v</sub> and PM<sub>2.5</sub>, WSOC, and Abs<sub>365</sub> in the  
 770 south and north of Beijing (\* indicates correlation is significant at the 0.05 level, and  
 771 \*\* indicates correlation is significant at the 0.01 level).

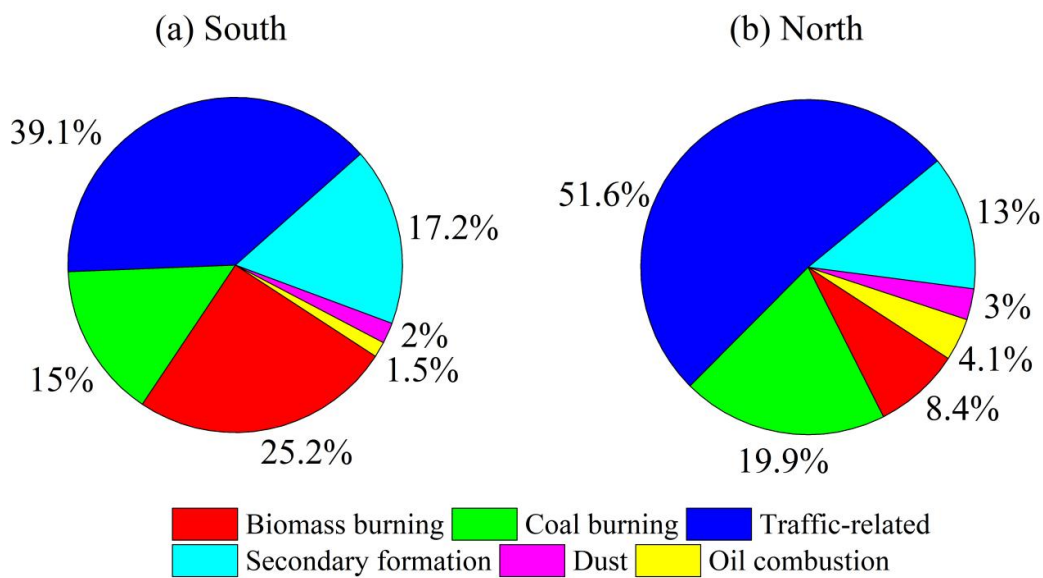
772



773

774 **Figure 4.** Correlation coefficients between  $DTT_v$  and elements in the (a) south and (b)  
 775 north of Beijing.

776



777

778 **Figure 5.** Contributions of resolved sources to  $DTT_v$  in the (a) south and (b) north of  
 779 Beijing.